SC5117.7TR

SC5117.7TR

Copy No. _____ 11

MICROSTRUCTURALLY DEVELOPED TOUGHENING MECHANISMS IN CERAMICS

TECHNICAL REPORT NO. 7

TRANSFORMATION TOUGHENING IN THE
Al_2O_3/ZrO_2 COMPOSITE SYSTEM

GENERAL ORDER NO. 5117
CONTRACT NO. N00014-77-C-0441

DOCUMENT NO. SC5117.7TR

Prepared for

D D C
RECEIVED
NOV 9 1979
B

F. F. Lange
Principal Investigator

OCTOBER 1979

DDC FILE COPY

Rockwell International
Science Center

79 11 08 071

REPORT DOCUMENTATION PAGE		READ INSTRUCTIONS BEFORE COMPLETING FORM
1. REPORT NUMBER	2. GOVT ACCESSION NO.	3. RECIPIENT'S CATALOG NUMBER
4. TITLE (and Subtitle) MICROSTRUCTURALLY DEVELOPED TOUGHENING MECHANISMS IN CERAMICS--Transformation Toughening in the Al2O3/ZrO2 Composite System. Al sub 2 O sub 3/ZrO sub 2		5. TYPE OF REPORT & PERIOD COVERED Technical Report 31 MAY 79 1 June 1978 — May 31, 1979
		6. PERFORMING ORG. REPORT NUMBER SC5117.7TR TR-7
7. AUTHOR(s) F.F. Lange		8. CONTRACT OR GRANT NUMBER(s) N00014-77-C-0441
9. PERFORMING ORGANIZATION NAME AND ADDRESS Rockwell International Science Center 1049 Camino Dos Rios P.O. Box 1085, Thousand Oaks, CA 91360		10. PROGRAM ELEMENT, PROJECT, TASK AREA & WORK UNIT NUMBERS NR 032-574 (471)
11. CONTROLLING OFFICE NAME AND ADDRESS Office of Naval Research 800 N. Quincy Street Arlington, VA 22217		12. REPORT DATE October 1979
		13. NUMBER OF PAGES 26
14. MONITORING AGENCY NAME & ADDRESS(if different from Controlling Office) Dr. R.C. Pohanka Office of Naval Research 800 N. Quincy Street Arlington, VA 22217		15. SECURITY CLASS. (of this report) Unclassified
		15a. DECLASSIFICATION/DOWNGRADING SCHEDULE

16. DISTRIBUTION STATEMENT (of this Report)

Approved for Public Release, Distribution Unlimited

17. DISTRIBUTION STATEMENT (of the abstract entered in Block 20, if different from Report)

18. SUPPLEMENTARY NOTES

19. KEY WORDS (Continue on reverse side if necessary and identify by block number)

Microstructure, Fracture Toughness, Martensitic Transformation, ZrO_2, Al_2O_3

20. ABSTRACT (Continue on reverse side if necessary and identify by block number)

Three Al_2O_3/ZrO_2 composites series, containing 0, 2, and 7.5 mole % Y_2O_3, respectively, were fabricated. For the $Al_2O_3/ZrO_2(+2m/oY_2O_3)$ series, tetragonal ZrO_2 was retained from one end-member to the other. Significant increases in fracture toughness and strength were observed for materials in this system. Strengths decreased with increasing temperature. These results are consistent with previous theoretical predictions.

DD FORM 1 JAN 73 1473   EDITION OF 1 NOV 65 IS OBSOLETE

389 949

TRANSFORMATION TOUGHENING IN THE Al_2O_3/ZrO_2 COMPOSITE SYSTEM

F. F. Lange

Structural Ceramics Group

Rockwell International Science Center
Thousand Oaks, CA.

ABSTRACT

Three Al_2O_3/ZrO_2 composite series, containing 0, 2, and 7.5 mole % Y_2O_3, respectively, were fabricated. For the $Al_2O_3/ZrO_2(+2m/oY_2O_3)$ series, tetragonal ZrO_2 was retained from one end-member to the other. Significant increases in fracture toughness and strength were observed for materials in this system. Strengths decreased with increasing temperature. These results are consistent with previous theoretical predictions.

SC5117.7TR

1.0 INTRODUCTION

A stress-induced, martensitic transformation can be used to increase
the fracture toughness of brittle materials based on ZrO_2.[1-6] Metastable,
tetragonal ZrO_2 is the toughening agent. Transformation to its stable,
monoclinic structure in the vicinity of the crack is responsible for the
increased fracture toughness.

A previous theoretical study[7] outlined the thermodynamics
concerning the general conditions required to retain tetragonal ZrO_2 and its
contribution to fracture toughness. One conclusion was the importance of the
elastic properties of the matrix material that constrains the shape change
associated with the transformation. That is, both the retension of the
metastable phase and its contribution to fracture toughness can be optimized
by increasing the elastic modulus of the matrix material. Based on this
conclusion, experimental study was directed toward two phase composites in
which tetragonal ZrO_2 could be incorporated into a polycrystalline matrix of
higher elastic modulus.

The Al_2O_3-ZrO_2 system was chosen for this study because Al_2O_3 has
approximately twice the elastic modulus of ZrO_2 (390 GPa vs 210 GPa) and both
phases are compatible with one another.[8] Claussen[9] has already
demonstrated that Al_2O_3/ZrO_2 polycrystalline composites could be fabricated
and, during the course of the present work, he[10] also demonstrated that
tetragonal ZrO_2 could be retained in Al_2O_3 in volume fractions up to 0.17.

2.0 EXPERIMENTAL

2.1   Fabrication and Phase Identification

The intent was to fabricate a series of Al_2O_3/ZrO_2 material from one end-member to the other and to retain ZrO_2 in its tetragonal structure. Initial studies indicated that within the range of fabrication parameters investigated, pure, tetragonal ZrO_2 could only be retained in volume fractions <0.15. Based on phase retentions studies in the ZrO_2-Y_2O_3 system,[6] additions of 2 mole % Y_2O_3 to the Al_2O_3/ZrO_2 composite powder were used to retain the tetragonal phase from one end-member to the other.

Three composite series were fabricated for this study: one containing pure ZrO_2 with volume fractions up to 0.20, one containing ZrO_2 + 2m/o Y_2O_3* in which tetragonal ZrO_2 was retained from one end-member to the other, and one containing ZrO_2 + 7.5m/oY_2O_3 in which cubic ZrO_2 was the second phase. The latter composite series was used for base line information where transformation toughening was not a phenomena associated with the material's mechanics.

Sub-micron powers were used.† Y_2O_3 was introduced as yttrium nitrate.§ Composite powders were mixed by ball-milling with methanol and Al_2O_3 balls in a plastic container. All powders were dried; those containing

---

*m/o = mole %, v/o = volume %
†Al_2O_3: Lindy B, Union Carbide Corp.; ZrO_2: Zircas Corp.
§Research Chemicals Inc.

yttrium nitrate were calcined at 400°C for 4 hrs. Densification was achieved
by hot-pressing. Most Y_2O_3 containing compositions were hot-pressed at
1600°C/2 hrs; compositions containing 0.8 and 1.0 volume fraction
$ZrO_2(+2m/oY_2O_3)$ were hot-pressed at 1400°C in order to achieve a smaller grain
size which allowed the retension of tetragonal ZrO_2. The non-yttria compo-
sites were hot-pressed at 1500°C, again to achieve a smaller grain size for
optimizing the retension of tetragonal ZrO_2. The pure Al_2O_3 end-member was
hot-pressed at 1400°C to achieve a grain size comparable to the two-phase
materials (the introduction of one end-member into the other limited grain
growth).

Archimedes' technique was used to measure density of the 5 cm
diameter hot-pressed billets. Specimens were cut, ground and polished* prior
to phase identification by x-ray diffraction analysis. Two-theta scans be-
tween 27° to 33° were used to estimate the tetragonal/monoclinic ZrO_2 ratio
and scans between 55° to 62° were used to confirm either the tetragonal or the
cubic ZrO_2 phase.

2.2   Mechanical Measurements

Young's modulus (E) of selected compositions was measured at room
temperature by the resonance technique in two modes of vibration: flexural
($9kH_3$) and extensional (60 kH_3).

---

*Surface damage caused by cutting and grinding causes the surface to
transform. Polishing decreases the depth of the transformed surface layer.

The critical stress intensity factor (K_c) was measured on polished specimens by using the indentation technique and the function

$$K_c = \frac{H\sqrt{d}}{3(H/3E)^{0.4}} \, f(c/d) \tag{1}$$

developed by Evans and Charles.[11] The hardness (H) was measured at a load of 20 kgm. The half-diagonal (d) of the pyramidal indent and half-crack length (c) were used with Young's modulus and the experimentally obtained function [11] [f(c/d)] to compute K_c. Three measurements were made for each material.

Flexural strength measurements were obtained in four-point bending (inner span: 1.22 cm, outer span: 2.54 cm) on diamond cut specimens (approximately 0.32 x 0.32 cm cross sectional) finished with a 220 grit diamond grinding wheel.

3.0 RESULTS

3.1 Fabrication and Phase Identification

Table 1 lists the fabrication conditions for the compositions reported here and their respective average properties. Densities of the $Al_2O_3/ZrO_2(+2m/oY_2O_3)$ materials obeyed the rule of mixtures for the end-members (Al_2O_3 and tetragonal ZrO_2); this indicated that theoretical density was achieved during fabrication. With the exception of the 60, 80, and 100% $ZrO_2(+2m/oY_2O_3)$ materials, tetragonal ZrO_2 was fully retained in this series. High proportions of tetragonal ZrO_2 could only be retained in the Al_2O_3/ZrO_2 (pure) series for volume fractions of $ZrO_2 < 0.10$.* The 20v/oZrO$_2$ composition in this series was friable, indicative of its high monoclinic content and suggestive of a highly microcracked material.

Figure 1 illustrates microstructures of polished surfaces typical of all the Al_2O_3/ZrO_2 compositions (cracks observed are those purposely propagated from the hardness indent). In general, the minor phase appears uniformly dispersed. The observed agglomeration of the minor phase in occasional groups of 2-5 grains indicates that the dispersion could be improved. The average grain size for the composite materials was dependent on the fabrication temperature, viz. ~0.2 µm at 1400°C, ~0.5 µm at 1500°C and ~1 µm at 1600°C. The

---

*It should be noted that phase identification was obtained from polished surfaces. Although polishing is effective in removing much of the damaged, transformed surface layer produced during machining, the tetragonal content of the subsurface material could be higher than reported in Table 1.

average grain size of the end-members hot-pressed at 1400°C was ~2 μm for Al_2O_3 and ~0.5 μm for ZrO_2.

3.2 Hardness

Figure 2 illustrates the Vickers (20 kgm) hardness as a function of composition, suggesting a linear rule of mixtures for the $Al_2O_3/ZrO_2(2m/oY_2O_3)$ series. The highly microcracked, $20v/oZrO_2$ (pure) composition is the exception to this behavior; its hardness is considerably less. Observations of the material adjacent to the hardness indent suggest that the indenter pushed the microcracked material aside as it extended into the surface.

3.3 Young's Modulus

Figure 3 reports the Young's modulus obtained from the two resonance techniques as a function of composition.

3.4 Critical Stress Intensity Factor

Figure 4 reports K_c as a function of composition for the three series of materials. The elastic modulus vs composition data shown in Fig. 3 was used with the experimental parameters (H,d,c) to compute K_c according to Eq.(1).

It should be pointed out here that the K_c values calculated for the Al_2O_3/ZrO_2 (pure) series (Fig. 4b) may be somewhat large due to the monoclinic contents of these materials. Namely, their monoclinic content suggests the

presence of microcracks that would lower Young's Modulus from those shown in Fig. 3, which were used to calculate K_c. As shown by Eq. (1), the relation between K_c and E is weak, e.g., a 20% decrease in E will only produce ~10% decrease in the calculated value of K_c. Thus, although the presence of monoclinic ZrO_2 in these materials might lower E (due to the presence of microcracks), the decrease in K_c from that reported is expected to be small. This effect is most significant for the 20% ZrO_2 (pure) composition where direct evidence for preexisting microcracks exists, viz. its friable nature and low hardness.

3.4   Strength

Flexural strength was determined as a function of composition for the $Al_2O_3/ZrO_2(+2m/oY_2O_3)$ series and as a function of temperature for the composition containing $23.9v/oZrO_2(+2m/oY_2O_3)$.

Strength vs composition results are plotted in Fig. 5. Specimens containing >45v/oZrO$_2$(+2m/oY$_2$O$_3$) were observed to contain one or two large through cracks of undetermined origin; strengths of these materials are not represented in Fig. 5. Results for strength vs temperature for the Al_2O_3/ZrO_2 (23.9v/o + 2m/oY$_2$O$_3$) material are illustrated in Fig. 6.

SC5117.7TR

4.0 ANALYSIS

4.1 Retension of Tetragonal ZrO_2

Theory[7] indicates that a critical size exists, below which a particle of tetragonal ZrO_2 can be constrained from transforming by an elastic matrix. The critical particle (or grain) size can be increased by increasing the elastic properties of the constraining matrix. In previous work,[6] a sufficiently small particle size could not be fabricated to retain pure, tetragonal ZrO_2 in a ZrO_2 constraining matrix. This work indicated that a particle size <0.2 μm would be required for a ZrO_2 constraining matrix. The current work has shown that pure, tetragonal ZrO_2 can be retained for an average particle size of 0.5 μm when the elastic modulus of the constraining matrix is increased to ~390 GPa (i.e., a composite of Al_2O_3 + small volume fractions of ZrO_2). A similar result has been obtained by Claussen.[10] Less of the tetragonal ZrO_2 is retained in the Al_2O_3/ZrO_2 (pure) series as the volume fraction of the ZrO_2 is increased. The increased ZrO_2 content decreases the elastic modulus of the composite and thus shifts the critical particle size to smaller values than those achieved during fabrication. These observations are consistant with the theory relating phase retension to the elastic properties of the constraining matrix.

Theory[7] also indicates that the critical size can be increased by increasing the differential chemical free energy ($\Delta G_{t \rightarrow m}^{chem}$) for $ZrO_2(t) \rightarrow ZrO_2(m)$ reaction. Alloying ZrO_2 with Y_2O_2 increases $\Delta G_{t \rightarrow m}^{chem}$ as evident from the lowering of the transformation temperature for Y_2O_3 additions up to eutectoid

composition at ~3m/o.[6] In the previous study, the critical grain particle size of tetragonal $ZrO_2(+2m/oY_2O_3)$ was determined to be 0.2 μm. The current study shows that the critical particle size can be increased to at least 1 μm with the higher elastic modulus of the Al_2O_3/ZrO_2 constraining matrix. Also note that as the $Al_2O_3/ZrO_2(+2m/oY_2O_3)$ composition approaches the ZrO_2 end-member, a large fraction of the tetragonal $ZrO_2(+2m/oY_2O_3)$ could not be retained by fabricating at 1600°C which produces a particle (or grain) size of 1 μm. In order to achieve a greater amount of phase retention, the fabrication temperature was decreased to 1400°C so that a grain size of 0.2 μm could be obtained. These observations are consistant with the theory[7] relating phase retention to the free energy change of the martensitic reaction.

4.2   Critical Stress Intensity Factor

A previous theoretical study[7] concerning the contribution of the stress-induced transformation to fracture toughness resulted in two expressions for the critical stress intensity factor, which represent the lower and upper bounds expected for K_c. The lower bound solution assumes that the transformation does not exhibit a stress hysteresis; this implies that the size of the process zone at the crack front is relatively independent of temperature. The expression for the lower-bound solution is

$$K_c^{\ell b} = [K_o^2 - A E_c V_d]^{1/2} , \tag{2}$$

where

$$A = 2\Delta G_{t \to m}^{chem} R / (1 - v_c^2) .$$

K_0 is the critical stress intensity factor for the composite material without the transformation, $\Delta G_{t \rightarrow m}^{chem}$ is the differential chemical free energy for the $ZrO_2(t) \rightarrow ZrO_2(m)$ reaction, E_c and v_c are Young's Modulus and Poisson's ratio for the composite, respectively, V_d is the volume fraction of the retained tetragonal ZrO_2 and R is the size of the process zone.

The upper bound solution assumes that the stress-induced transformation at the crack front is irreversible due to a stress hysteresis effect. With this assumption, the size of the process zone (r) depends on temperature and K_0. The upper bound K_c solution has the form

$$K_c^{ub} = K_0 (1 + B E_c V_p)^{-1/2} \tag{3}$$

where

$$B = \frac{2 \Delta G_{t \rightarrow m}^{chem} (\frac{\Delta V}{V})^2}{[2\pi (1 - v_c^2) \Delta G_{t \rightarrow m}^{chem} + U_{se}^0]^2} .$$

U_{se} is the strain energy and $\Delta V/V$ is the volume change associated with the transformation.

Comparisons of the upper and lower bound solutions with the experimental data were made by calculating the constants A and B in Eqs (2) and (3), respectively, by using the experimental data for the $45v/oZrO_2$ $(+2m/oY_2O_3)$ composition. These constants were used along with the experimental E_c (Fig. 3) and K_0 (Fig. 4a) for the $Al_2O_3/ZrO_2(7.5m/oY_2O_3)$ series to calculate K^{ub} and K^{lb} as a function of V_p. As seen in Fig. 4, the lower bound solution agrees with the experimental data for $V_p < 0.6$.

Further comparison can be made with the lower bound solution by using Whitney's [12] thermodynamic data for pure ZrO_2. By assuming the same value of $\delta\Delta G/\delta T$ reported by Whitney for pure ZrO_2 and an unconstrained transformation temperature of 800°C for the $ZrO_2(+2m/oY_2O_3)$, $\Delta G_{t \to m}^{chem}$ (25°C) = -193 x $10^6 J/m^3$. Substituting this value into Eq. (2) along with the other experimental factors, the radius of the process zone (R) is calculated to be 1 μm. This calculation suggests that the transformation depth on the crack surface is 1 μm which is the approximate particle size of the retained, tetragonal ZrO_2 in these materials. The agreement between the calculated zone size and the particle size adds some confidence to the theoretical results for the lower bound solution.

The maximum in the K_c data for the Al_2O_3/ZrO_2 (pure) series can be explained by the decreasing retension of tetragonal ZrO_2 for $V_{ZrO_2} > 0.10$. That is, the maximum K_c was obtained for the composition in which the retension was a maximum. Claussen[9] also observed maximum in his K_c data for two series of Al_2O_3/ZrO_2 (pure) materials over a similar range of V_{ZrO_2}. For his data, the maximum K_c shifted to a higher volume fraction for the smaller particle size series where greater retention of the tetragonal phase is expected from theory. From these observations, it can be concluded that tetragonal ZrO_2 is the toughening agent and K_c can be optimized by retaining the maximum content of this phase.

4.3   Strength vs Composition

The strength data presented in Fig. 5 has been analyzed to determine its dependence on the experimental K_c values. In this analysis, it was assumed that the crack size distribution responsible for failure remained unchanged from material to material. With this assumption, the strength of each material should be related by their respective critical stress intensity factors:

$$\sigma_2 = (\frac{K_2}{K_1})\sigma_1 \quad . \tag{4}$$

This relation was used with the average strength and K_c for the pure Al_2O_3 to obtain the broken line in Fig. 5. As shown, three of the original five sets of data were in good agreement with this analysis, but two of the data sets (viz V_p = 0.182 and 0.295) were higher than predicted.

Pascoe and Garvie[13] have shown that surface compressive stress arises in materials containing metastable, tetragonal ZrO_2 when the transformation at the surface is induced by an abrasion process. The volume increase assciated with transformed surface layer gives rise to the compressive stresses. Since each set of strength specimens was independently surface ground, it was suspected that several of these sets (the two that resulted in the higher values) may have received surface damage to imparted sufficient surface compressive stresses to increase their strength. To test this hypothesis, a small task was initiated to examine the effect of surface abrasion on strength. Although the principal results of this task will be reported

elsewhere,[14] it was shown that if the abrasively ground specimens were annealed at 1300°C to eliminate the transformed surface layer, the average strength was lowered to that expected from Eq. (4). These data are shown by the open triangle in Fig. 5.

It can be concluded that the strength of the $Al_2O_3/ZrO_2(+2m/oY_2O_3)$ composite materials increases proportionally to their increase in K_c as expected. Additional strengthening can be obtained by compressive stressing the surfaces through abrasion. Studies are currently underway to characterize and optimize the abrasion phenomena.

4.4   Strength vs Temperature

Strength data in Fig. 6 were analysed in the same manner as described by Eq. (4). Eq.(2) was used to obtain K_c as a function of temperature. Whitney's results [12] for $\Delta G_{c \rightarrow m}^{chem}$ vs temperature for pure ZrO_2 were used to determine the temperature dependence of the factor A in Eq. (2) with an assumed unconstrained transformation temperature of 800°C for ZrO_2 $(+2m/oY_2O_3)$. The results of this analysis are represented as the solid line in Fig. 6.

As shown in Fig. 6, the lower bound solution for K_c results in near perfect agreement with strength vs temperature data over the range of 25° to 1000°C. At temperatures <25°C, agreement is poor - which may be due to either an increase process zone size at these lower temperatures (suggesting that the

SC5117.7TR

upper bound K_c solution may be valid at lower temperatures) or some other currently unexplained reason.

5.0 CONCLUSIONS

It has been demonstrated that the critical stress intensify factor and the strength of polycrystalline Al_2O_3 can be significantly increased by incorporating tetragonal ZrO_2. Fabrication conditions required to retain the tetragonal phase at room temperature indicate a critical particle size must not be exceeded. The critical particle size appears to be related to the elastic properties of the constraining matrix and the alloy additions to ZrO_2 as indicated by theory.

The fracture toughness is related to the amount of retained tetragonal phase, i.e., tetragonal ZrO_2 is the toughening agent. When the present data are compared to similar data obtained for the ZrO_2(cubic)/ZrO_2 (tetragonal) composite series,[6] it can be shown that greater gains in K_c are observed with the higher elastic modulus of the Al_2O_3/ZrO_2 constraining matrix as predicted by theory. Although more fundamental thermodynamic data and direct measurements of the process zone size are needed, the current K_c and strength data indicate that the process zone size is independent of composition and temperature.

Regardless of the views expressed relating theory and experiment, it should be noted that materials fabricated for this study are some of the strongest ceramics and that surface abrasion is not detrimental. These bottom line results strongly suggest that transformation toughening should be pursued for other systems within the framework of present and improved theoretical direction.

REFERENCES

1. R. C. Garvie, R. H. Hennick and R. T. Pascoe, Nature 258, 703 (1975).

2. R. C. Garvie and R. T. Pascoe, Processing of Crystalline Ceramics, ed. by H. Palmour III, R. F. Davis and T. M. Hare, p. 263, Plenum Press (1978).

3. D. L. Porter and A. H. Heuer, J. Am. Ceram. Soc. 60, 183 (1977); ibid. 280 (1977).

4. T. K. Gupta, J. H. Bechtold, R. C. Kuznichi, L. H. Cadoff and B. R. Rossing, J. Mat. Sci. 12, 2421 (1977).

5. T. K. Gupta, F. F. Lange and J. H. Bechtold, J. Mat. Sci. 13, 1464 (1978).

6. F. F. Lange, "Transformation Toughening in the ZrO_2(Cubic)/ZrO_2 (tetragonal) Composite System," to be published: ONR Rept #3, Contract N00014-77-C-0441, July 1978.

7. F. F. Lange, "Stress-Induced Phase Transformations: Theory of Phase Retension and Fracture Toughness," ONR Rept #6, Contract N00014-77-C-0441, Oct. 1979.

8. E. M. Levin, C. R. Robbins, and H. F. McMurdie, "Phase Diagrams for Ceramists, 1969 Supplement," The American Ceramic Soc., 1969.

9. N. Claussen, J. Am. Ceram. Soc. 59 [1-2], 49 (1976).

10. N. Claussen, ibid 61 [1-2], 85 (1978).

11. A. G. Evans and E. A. Charles, J. Am. Ceram. Soc. 59 [7-8], 371-2 (1976).

12. E. D. Whitney, J. Am. Cerma, Soc. 45, 612 (1962).

13. R. T. Pascoe and R. C. Garvie, "Ceramic Microstructures '76," ed by R. M. Fulrath and J. A. Pask, Westview Press p.774, 1977.

14. D. J. Green and F. F. Lange, to be published.

Rockwell International
Science Center

SC5117.7TR

ACKNOWLEDGEMENTS

TABLE I

FABRICATION CONDITIONS, PHASE CONTENT AND PROPERTIES OF Al_2O_3/ZrO_2 COMPOSITES

v/o ZrO_2	m/o Y_2O_3	Fabrication Condition	Density (gm/cm^3)	% ZrO_2* phrase	H (GPa)	E (GPa)	Kc ($MPa\ m^{1/2}$)
$Al_2O_3/ZrO_2(+2m/oY_2O_3)$ Series							
0	-	1400°C/2hr	3.98	-	17.6	390	4.89
6	2	1600°C/2hr	4.12	100t	16.8	-	5.97
12.3	2	1600°C/2hr	4.26	100t	15.9	-	6.22
18.2	2	1600°C/2hr	4.38	100t	16.1	356	6.58
23.9	2	1600°C/2hr	4.50	100t	16.4	-	6.38
29.5	2	1600°C/2hr	4.62	100t	15.7	-	7.43
45.0	2	1600°C/2hr	4.89	tr m	15.1	291	8.12
60.0	2	1600°C/2hr	5.24	~95t	13.7	-	7.45
80.0	2	1400°C/2hr	5.57	~85t	12.6	237	6.79
100.0	2	1400°C/2hr	6.01	~80t	11.6	210	6.62
Al_2O_3/ZrO_2(pure) Series							
7.5	-	1500°C/2hr	4.12	~90t	17.2	-	5.88
10.0	-	1500°C/2hr	4.15	~80t	15.8	-	6.73
12.5	-	1500°C/2hr	4.22	~70t	16.9	-	6.21
15.0	-	1500°C/2hr	4.25	~50t	17.3	-	5.71
20.0	-	1600°C/2hr	-	<20t	10.1	-	(5.25)
$Al_2O_3/ZrO_2(+7.5m/oY_2O_3)$ Series							
20.0	7.5	1600°C/2hr	4.46	100c	15.8	-	4.54
40.0	7.5	1600°C/2hr	4.89	100c	15.9	-	3.75
60.0	7.5	1600°C/2hr	5.28	100c	15.0	-	3.50
80.0	7.5	1600°C/2hr	5.63	100c	14.3	-	3.14
100.0	7.5	1600°C/2hr	5.95	100c	11.4	-	3.90

t = tetragonal
c = cubic
trm = trace monoclinic

18

FIGURES

Fig. 1   SEM micrographs of polished surfaces of $Al_2O_3/ZrO_2(+2m/oY_2O_3)$ composites at ZrO_2 volume fractions of 0.063, 0.123, 0.45 and 0.80. Al_2O_3 is dark phase.

Fig. 2   Vicher's Hardness (measured at 20 kgm) for the true composite series.

Fig. 3   Young's Modulus vs composition for the $Al_2O_3/ZrO_2(+2m/oY_2O_3)$ series.

Fig. 4   a) Critical stress intensity factor vs composition for the $Al_2O_3/ZrO_2(+2m/oY_2O_3)$ (circles) and the $Al_2O_3/ZrO_2(+7.5m/oY_2O_3)$ series (squares).

         b) Critical stress intensity factor vs composition for the $Al_2O_3/ZrO_2(pure)$ series.

Fig. 5   Flexural strength vs composition for the $Al_2O_3/ZrO_2)+2m/oY_2O_3)$ series.

Fig. 6   Flexural strength vs temperature for the $Al_2O_3/ZrO_2(25.9$ v/o $+ 2m/oY_2O_3)$ material.

6 V/o　　　　12 V/o

2 um

45 V/o　　　　80 V/o

Fig. 1

SC5117.7TR

SC79-5969

Fig. 2

21

SC5117.7TR

SC79-5968

Fig. 3

22

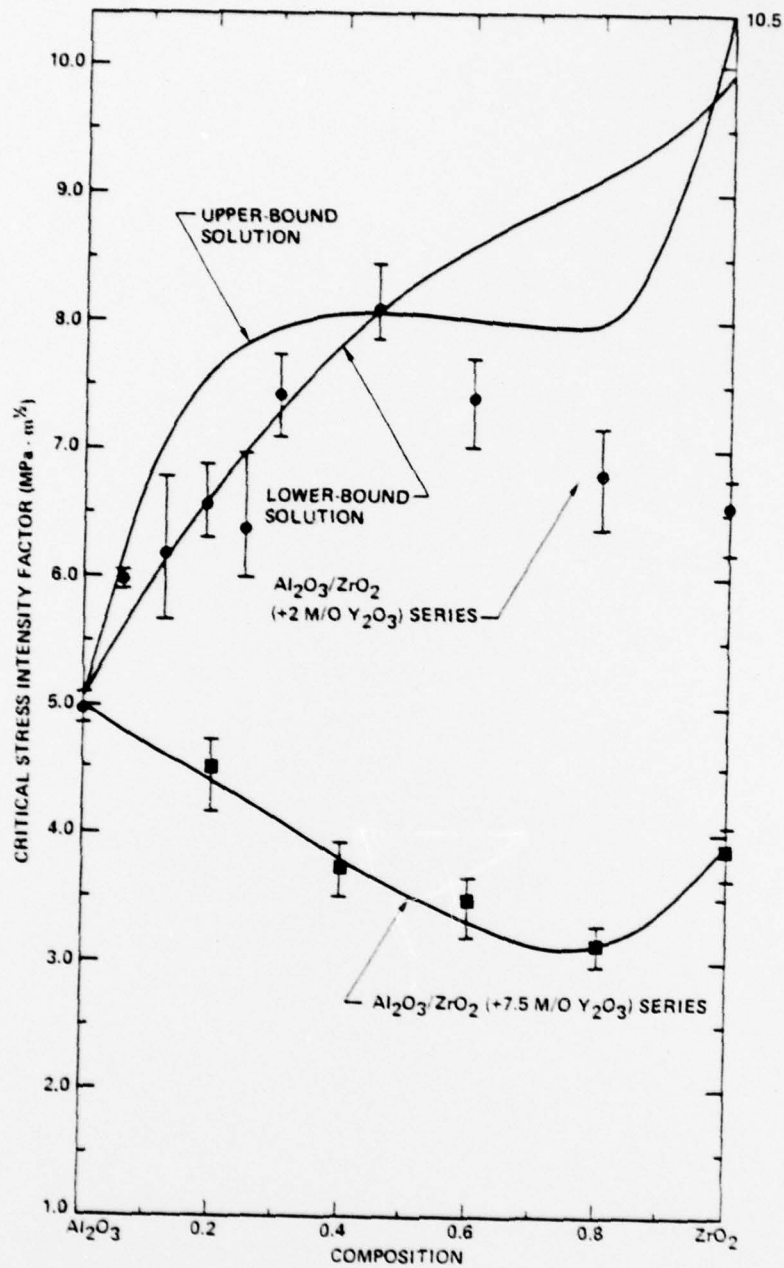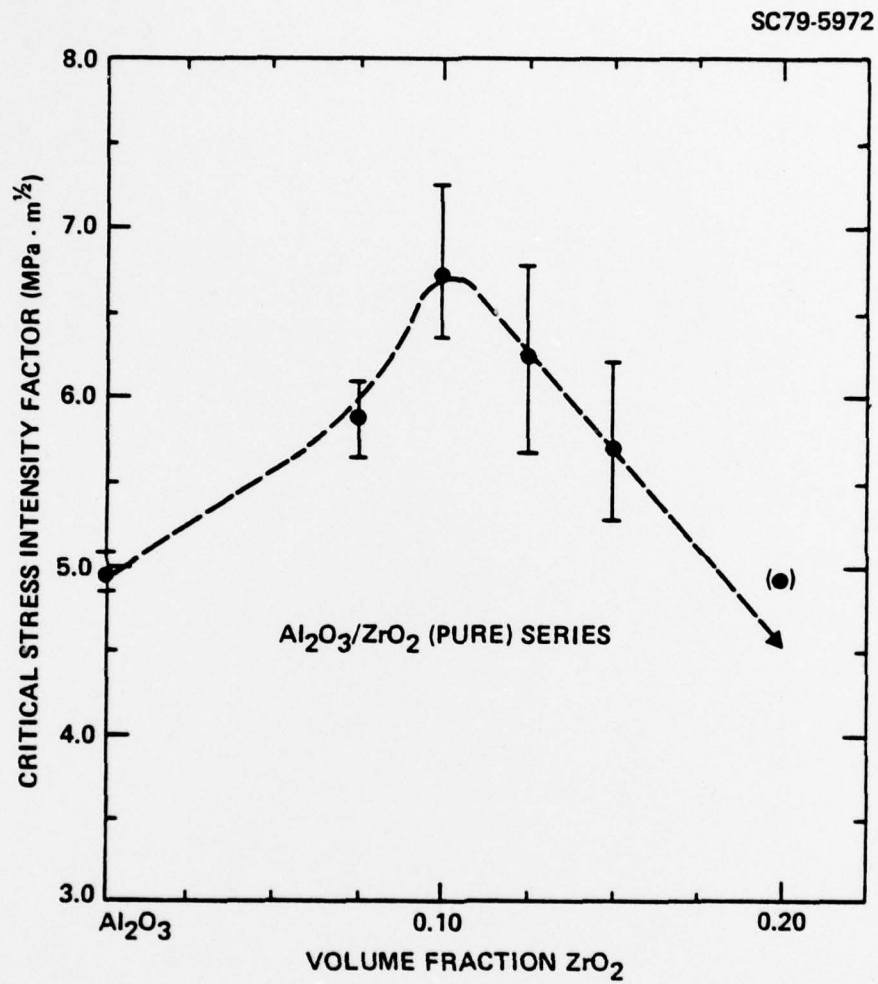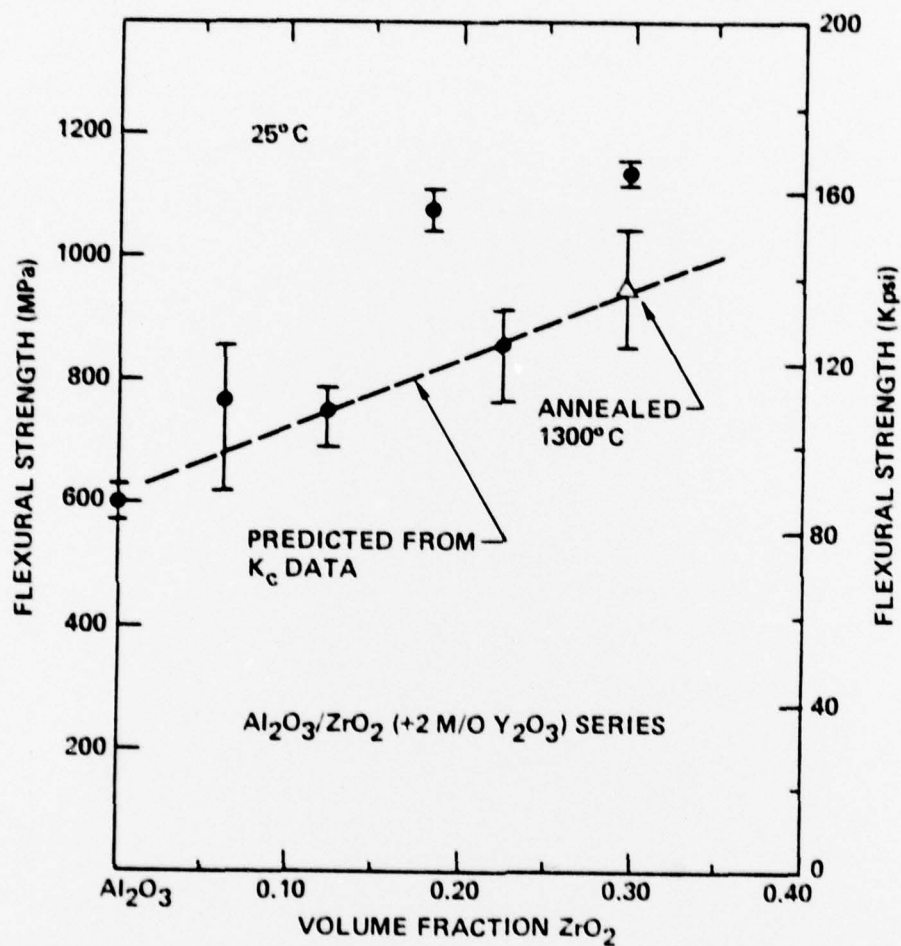SC79-5970

Fig. 4a

SC79-5972

Fig. 4b

SC79-5971

Fig. 5

Fig. 6

26